

## Planimetric offset adjustment of multitemporal laser scanner data

Mariano García<sup>1</sup>, Elena Prado<sup>2</sup>, David Riaño<sup>3,4</sup>, Emilio Chuvieco<sup>1</sup> and Mark Danson<sup>5</sup>

<sup>1</sup> Department of Geography, University of Alcalá. Alcalá de Henares, 28801. Madrid (Spain).

[mariano.garcia@uah.es](mailto:mariano.garcia@uah.es) ; [emilio.chuvieco@uah.es](mailto:emilio.chuvieco@uah.es)

<sup>2</sup> Remote Sensing Area, National Institute of Aerospace Technology (INTA), Crta. de Ajalvir Km 4, 28850 Torrejón de Ardoz, Madrid [pradooe@inta.es](mailto:pradooe@inta.es)

<sup>3</sup> Institute of Economics and Geography, Spanish National Research Council (CSIC), Albasanz 26-28 28037 Madrid (Spain). [driano@ieg.csic.es](mailto:driano@ieg.csic.es)

<sup>4</sup> Center for Spatial Technologies and Remote Sensing (CSTARS), University of California, 250-N, The Barn, One Shields Avenue, Davis. CA 95616-8617, USA

<sup>5</sup> Centre for Environmental Systems Research, School of Environment and Life Sciences, University of Salford, Manchester M5 4WT, UK.

### Abstract

LiDAR (Light Detection and Ranging) data have shown a great potential for 3D modelling applications. This potential lies on the ability of LiDAR systems to generate highly dense 3D point clouds for describing the terrain surface. Several error sources affect the position accuracy of the 3D points, which are represented as offsets between the overlapping areas. Several methods have been developed to correct these displacements using height or intensity data. This paper proposes a three steps procedure to correct the offset observed between a multitemporal dataset. Firstly intensity images were generated. Secondly, an area based image correlation technique was applied to extract evenly distributed control points. Finally the control points were used to determine the parameters of a global transformation by least squares. The technique showed good performance for the study area reducing significantly the planimetric discrepancies observed.

*Keywords: LiDAR, planimetric adjustment, image matching, least squares*

### 1. Introduction

LiDAR (Light Detection and Ranging) data have shown a great potential for several applications such as generation of Digital Terrain and Surface Models (DTM and DSM), generation of 3D object models, forest inventory, etcetera (Maas and Vosselman, 1999; Næsset *et al.*, 2004). This potential lies on the ability of LiDAR systems to generate highly dense 3D point clouds which describe the terrain surface. Therefore, 3D modelling will be influenced by the accuracy with which the coordinates (X, Y, Z) of the point cloud are determined.

In the case of digital terrain model applications the height accuracy is the most important factor to take into account; however, in other 3D modelling applications discrepancies in the Z coordinate as well as in X and Y coordinates have to be determined (Maas, 2001). A wide variety of error sources affect the position accuracy of the 3D points, which in general terms can be grouped into: alignment errors, precision of range determination, errors of the scanning mirror, and GPS/INS system (Huising and Gomes Pereira, 1998; Maas, 2001). The latter commonly accounts for the largest errors, with errors up to 10 to 20 centimetres in the height and 50 centimetres in planimetry (Maas, 2001). These errors are represented as offsets or discrepancies between the overlapping areas of adjacent or crossing strips in relative terms or as offset at ground control points in absolute terms. Special attention has been paid to the relative adjustment of overlapping strips. As a result, several procedures have been suggested to overcome those displacements (Crombaghs *et al.* 2000; Maas, 2001; Vosselman, 2002a; Pfeifer

*et al.*, 2005).

Pfeifer *et al.* (2005) grouped the methods into those that only consider the observed discrepancies between the points from two adjacent strips, and those methods that are based on a model of the sensor system relating each point to its original observation. Sensor-based models have the main advantage that allow to assessing the true problem and not merely cope with the phenomena (Kager, 2004). Kager (2004) proposed a method for simultaneous 3-D fitting of laser data applying correction polynomials to the registered orientation elements as a function of time. Tie-features were used for the block adjustment. The main limitation for the application of sensor-based methods is that require data that are not usually available to end-users. Thus, several methods which consider the discrepancies between points from adjacent strips have been proposed. Pfeifer *et al.* (2005) proposed a method that used tie surfaces through segmentation of the LiDAR data into planar patches. Subsequently the segments were judged according to quality and distance criteria. Finally, Comparison of the height of one segment to a plane formed by the points in the adjacent strip(s) allowed determination of height offset.

Other researchers propose to use linear features, which simplify the processing and increase the accuracy, such as gable roofs or ditches to measure the strip shifts (Vosselman, 2002a; Lee *et al.* 2007). Lee *et al.* (2007) proposed a 5-steps algorithm where planimetric offset are determined first and subsequently the height is corrected. The algorithm implies generation of a data structure (Triangular Irregular Network, TIN), segmentation of points into planar patches (e.g. roofs), determination of the intersection line between planar patches, distance measurement between lines, and application of a global transformation to correct the data.

Maas (2000) presented a procedure to precisely determine strip discrepancies in all three coordinate directions, based on least squares matching applied to LiDAR data in a TIN structure. In this method, several patches were selected. The height of a given point in one of the strips was compared to the height of points of the other strip interpolated in the TIN mesh at the same location. This difference gave an observation equation that was used to determine the shift parameters. The TIN structure has the advantage that non-interpolated raw data are used, avoiding the bias introduced by grid interpolation in occlusion areas. However, despite the advantages of a TIN structure over an interpolated grid, the method required patches containing significant height contrast in orthogonal coordinate directions. In regions where this requirement is impossible or difficult to fulfil, intensity images can be used for planimetric shift determination using matching techniques (Maas, 2001; Maas 2002; Vosselman, 2002b). Image matching is commonly applied in photogrammetry and airborne remote sensing for the establishment of correspondence between images. The methods used in image matching can be grouped into: Intensity or area based methods, feature based methods and relational methods (Lerma, 2002).

Though the methods afore mentioned have been applied to the adjustment between adjacent and crossing strips, they could be applied to a multitemporal LiDAR dataset of a given area in the same manner. Also, the methods have been developed for areas where linear or surface elements such as gable roofs, roads or ditches are easier to extract. This paper shows the utility of area-based matching applied to intensity images to estimate and correct the planimetric offset between two dataset acquired over a complex forested area in Spain, where the application of feature-based techniques is difficult. A three steps procedure was applied to extract evenly distributed control points by an area based image correlation technique, which are then used to determine the parameters of a global transformation by least squares.

## 2. Methods

### 2.1. Study area and data set

This study was carried out over a forested area located in the Natural Park of “Alto Tajo” in Guadalajara, Central Spain (UL: 40° 56' 49" N; 2° 14' 49" W; LR: 40° 48' 25" N; 2° 13' 21" W). The area is characterized by a high diversity of species, mainly pines (*Pinus sylvestris* L., *Pinus nigra* Arn., *Pinus pinaster* Ait.) and oaks (*Quercus faginea* Lam., *Quercus ilex* L and *Quercus pyrenaica* Willd.). The mean height of the study area is 1200 m, with a maximum height of 1403 m and a minimum height of 895 m.

The study area was flown twice at the end of the spring of 2006, in May 16<sup>th</sup> and June 3<sup>rd</sup>. with an Optech 3033 LiDAR system. The flying height was 2050 m above mean sea level with a maximum scan angle of  $\pm 12^\circ$ , a point density of approximately 2.3 points/m<sup>2</sup>. The dataset consists of 3 strips flown in north-south direction with no overlap, and a crossing strip for calibration purposes, covering an area of approximately 382 Km<sup>2</sup>. The data available included X, Y and Z coordinates in UTM-zone 30 (WGS84), both first and last returns, and the intensity of each return.

Inspection of the relative adjustment between the two LiDAR flights showed a good relative fitting in the Z direction but revealed a systematic offset in the XY direction. Therefore, in order to determine the magnitude of this displacement and to correct it, an image matching technique was applied to the intensity images generated from the laser data and subsequently a global transformation was used.

### 2.2. Planimetric offset determination

In the previous section several methods proposed to correct the offset between LiDAR datasets have been described. Most of the methods were developed for urban areas, using linear features or surface elements to determine shift in the three coordinates. Our study area, with very few gable roofs (only in one strip out of three) or linear elements, hampered the application of feature-based methods. In addition the main objective of this study was to correct the planimetric offset of the datasets. Thus, an area based correlation technique was applied to the intensity images. The method presented in this paper was carried out in three steps. Firstly, intensity images were created from the point cloud data. Second, an area-based method was applied over each strip to extract sufficient number of control points. Subsequently, the extracted control points were used to derive the parameters of a global transformation by least squares.

#### 2.2.1. Generation of intensity images

Application of an area based matching requires the generation of a raster from the irregularly distributed point cloud, so the grey-level or digital number (DN) distribution of the two images can be compared. Therefore, the original point data were interpolated into a grid with a spatial resolution of 0.5m, using a normal core interpolation method. This method uses the intensity values for a given number of points within a defined radius that defines the interpolation area. A 2 m radius was used for the interpolation area. The interpolated values are calculated based on a distance weighted average. The weighting function decreases as an exponential function of the distance (Wyseman, PCI Geomatics, personal communication). Since intensity images presented a clear speckle noise, a median filter was applied to reduce its effect over the matching process (figure 1).



Figure 1: Intensity image generated using normal core interpolation (left) and intensity image filtered using a median filter (right)

### 2.2.2. Planimetric offset determination

The basic assumption of area based methods for image matching is that homologous pixels have similar radiometric (or intensity in LiDAR data) values. Area based control points extraction methods search to optimize a predefined objective function, defined by a similarity measure such as correlation coefficient, normalized cross correlation, or mutual information, based on template matching (Liu *et al.* 2006). The template can be the whole of the image or a subset.

Determination of the planimetric offset was carried out using a routine developed by Prado (2007). This routine computes the correlation coefficient between two  $M \times N$  matrices. One of these matrices is established as the reference window (master), while the other matrix (slave) is moved vertically and horizontally over the master. The size of these windows was set to 100x100 pixels. Thus, the images were divided in subsets of 100x100 pixels. For each subset the slave window was moved over the master (up to  $\pm 3$  pixels) and the correlation coefficient ( $r$ ) was computed. As a result the routine provides an image where the DN value represents the maximum correlation coefficient ( $r$ ) found, and two images where each pixel represents the shift in X and Y that made maximum the correlation coefficient. These images allow detecting the existence of a given pattern in the distribution of the X and Y offsets. Also, since the images are divided in subsets of 100x100 pixels, the error can be evaluated locally, mapping the offset along the whole of the strips.

Usually, since it is very difficult to obtain a maximum value in the correlation process ( $r=1$ ) a minimum threshold is established to accept a point, for example  $r=0.5$  (Lerma, 2002). In this study, a threshold of  $r=0.8$  was applied to the correlation values obtained, in order to extract the definite control points to be later used in the determination of the parameters of the global

model by least squares. Also a regular grid was created and overlaid to the correlation images. Thus, only those points of the grid that laid over pixels with a correlation value equal or greater than 0.8 were used as ground control points. This made it possible to extract evenly distributed control points over the overlapping area along the strips.

### 2.2.3. Transformation model determination

The control points previously extracted were used to calculate the coefficients of the global function to be applied. Approximately 85% of the extracted points were used as control points; the remaining 15% was used as validation points. Since the displacements observed over the overlapping area did not show local deformations (figure 2), a 2D affine transformation was applied to correct the planimetric offset between the intensity images. This geometric transformation, was applied to the LiDAR June 3<sup>rd</sup> data to match with May 16<sup>th</sup> data.

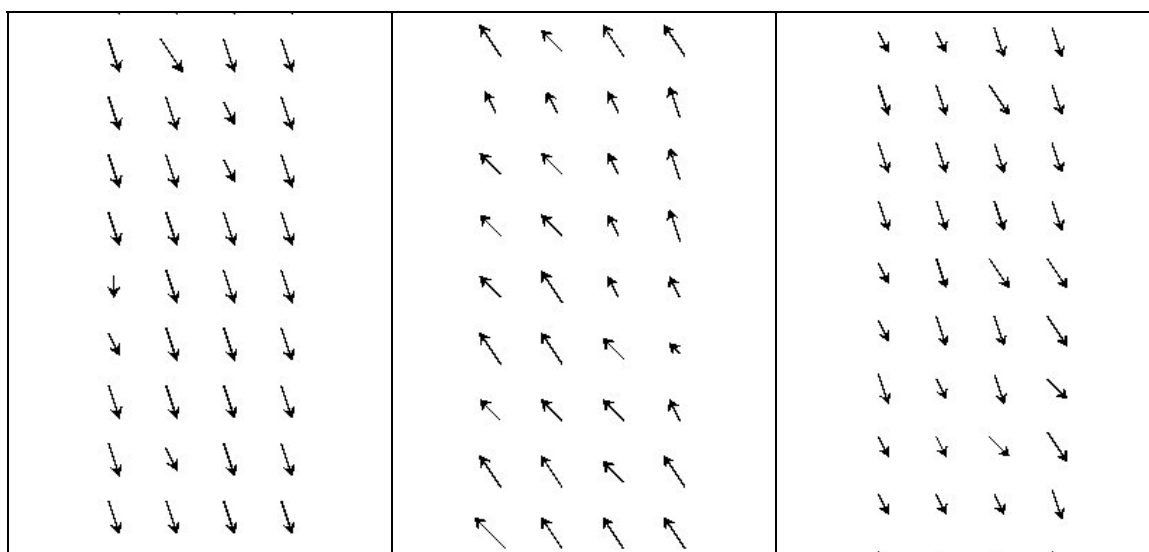


Figure 2: Subsets of the vector plots that show the pattern of the planimetric offset observed for the three strips. From left to right 1f-1s; 2f-2s; 3f-3s (1f, 2f, 3f: refers to the first day flight; 1s, 2s, 3s: refers to the second day flight)

The mathematical model of the affine transformation can be represented as:

$$\begin{pmatrix} X' \\ Y' \end{pmatrix} = \begin{pmatrix} a & b & c \\ d & e & f \end{pmatrix} \begin{pmatrix} X \\ Y \\ 1 \end{pmatrix} \quad (1)$$

Where a, b, c, d, e, and f represent the geometric parameters of the transformation, (X', Y') are the transformed coordinates and (X Y) are the observed coordinates, both in the UTM 30-WGS84 system.

### 3. Results

The routine applied to determine the planimetric offset, produced three new images, namely the correlation coefficient, the X-shift ( $\square X$ ) and the Y-shift ( $\square Y$ ) where the correlation found

reached a maximum. Table 1 presents the mean correlation coefficients computed for each strip (the mean value was computed for all pixels of the correlation images, not only for those having a correlation value higher than the threshold applied). It also presents the maximum displacements ( $\Delta X_{max}$ ,  $\Delta Y_{max}$ ) found at the control and validation points, and the number of control points and validation points used in each case. As can be seen from this table, the offset was higher for the Y coordinate than the X coordinate. Also, the sign of the error changed according to the direction of the flight, i.e. the first and the third strip were flown in the same direction N-S while the second was flown in an S-N direction. A slightly lower correlation coefficient was found for the first strip, since the characteristics of the area covered by this strip made more difficult to perform the matching. The number of control points found in the first strip was nearly half of the number of points extracted in the other two strips.

Table 1: Correlation coefficients and control points extraction (\*1f, 2f, 3f: refers to the first day flight; 1s, 2s, 3s: refers to the second day flight)

Strip *	Mean Correlation Coefficient	Control Points	Check Points	$\Delta X_{max}(m)$	$\Delta Y_{max}(m)$
1f-1s	0.48	40	7	-1	1.5
2f-2s	0.55	82	12	1	-1.5
3f-3s	0.54	94	14	-1	1.5

Table 2 shows the geometric parameters of the 2D affine transformation obtained from least squares, which were subsequently applied to the original data sets.

Table 2: Geometric parameters of the 2D affine transformation

Strip *	a	b	c	d	e	f
1f-1s	0.999404	$6.603 e^{-6}$	0.0054	-0.0001175	0.999986	-0.0223
2f-2s	0.999930	$-8.749 e^{-6}$	-0.0028	-0.001187	1.0000107	0.0146
3f-3s	0.998103	$-2.1434 e^{-5}$	0.0003	0.0002042	0.9999997	-0.0166

When applying these parameters to the check points the offsets were reduced considerably. Thus for the first strip the root mean square error (rmse) in X and Y before correcting the shifts were 0.46 m and 1.41 m respectively, whereas after applying the 2D affine transformation the rmse were 0.24 m in X and 0.33 m in Y. For the second strip similar results were obtained, with an rmse for the X coordinate of 0.56 m and 1.45 m for the Y coordinate before the correction, and after the affine transformation the rmse in X was 0.24 m and 0.27 m in Y. Finally for the third strip the results were,  $rmse-X=0.55$  m and  $rmse-Y=1.29$  m before correction, and after applying the transformation model the  $rmse-X$  and the  $rmse-Y$  were reduced to 0.23 m and 0.30 m respectively.

Figure 3 shows a subset of one of the strips before and after correcting the planimetric offset observed. It can be seen that the datasets show a systematic shift in the horizontal plane, and that this displacement is corrected after applying the 2D affine transformation.

After correcting the X,Y offset, it was verified the relative fitting of the data in the Z direction. Thus, a flat area with sparse vegetation was selected from each strip, and a DTM was generated for those areas. Subsequently, the DTMs generated for the second flight (before and after the correction) were compared to the DTMs generated for the first flight. Table 3 shows the mean and the standard deviation of the absolute differences between the DTMs generated.

Table 3: Verification of the Z adjustment before and after the planimetric correction

Strip *	□□Z  Before		□□Z  After	
	Mean	Standard deviation	Mean	Standard deviation
1f-1s	0.058	0.043	0.073	0.044
2f-2s	0.056	0.050	0.066	0.050
3f-3s	0.140	0.100	0.070	0.060

Similar values were obtained for the first and second strips. The highest difference was observed for the third strip, where the mean difference after the affine transformation was reduced from 14 cm to 7 cm. This could be explained because the area used in this strip presented a certain feature and, therefore the planimetric offset influenced the vertical component.

#### 4. Conclusions

Throughout this paper it was demonstrated that application of image matching techniques to intensity images interpolated from the 3D point cloud, can be useful to determine the planimetric offset observed between two LiDAR flights carried out over a forested area, especially when feature-based techniques are difficult to implement due to the lack of linear features. Correction of this displacement it is important when performing a multitemporal study or even to increase the point density by merging the data from the two flights when they are carried out close in time. Point density has shown to be more important than other variables as the footprintsize, in determining certain forest variables as crown area and volume area (Goodwin et al., 2006)

Though in the case of a global deformation, as it was the one observed for our data, an optimal matching leads to the final transformation model without explicitly generating the control points (Liu *et al.* 2006), the two step approach used here (extraction of control points and determination of transformation parameters by least squares) would allow to detect more complex local deformations. In such a case, local transformation as for example piecewise linear models or local weighted mean model could be applied. These methods usually need a large number of evenly distributed control points since the parameters of the transformation vary across different regions over the image.

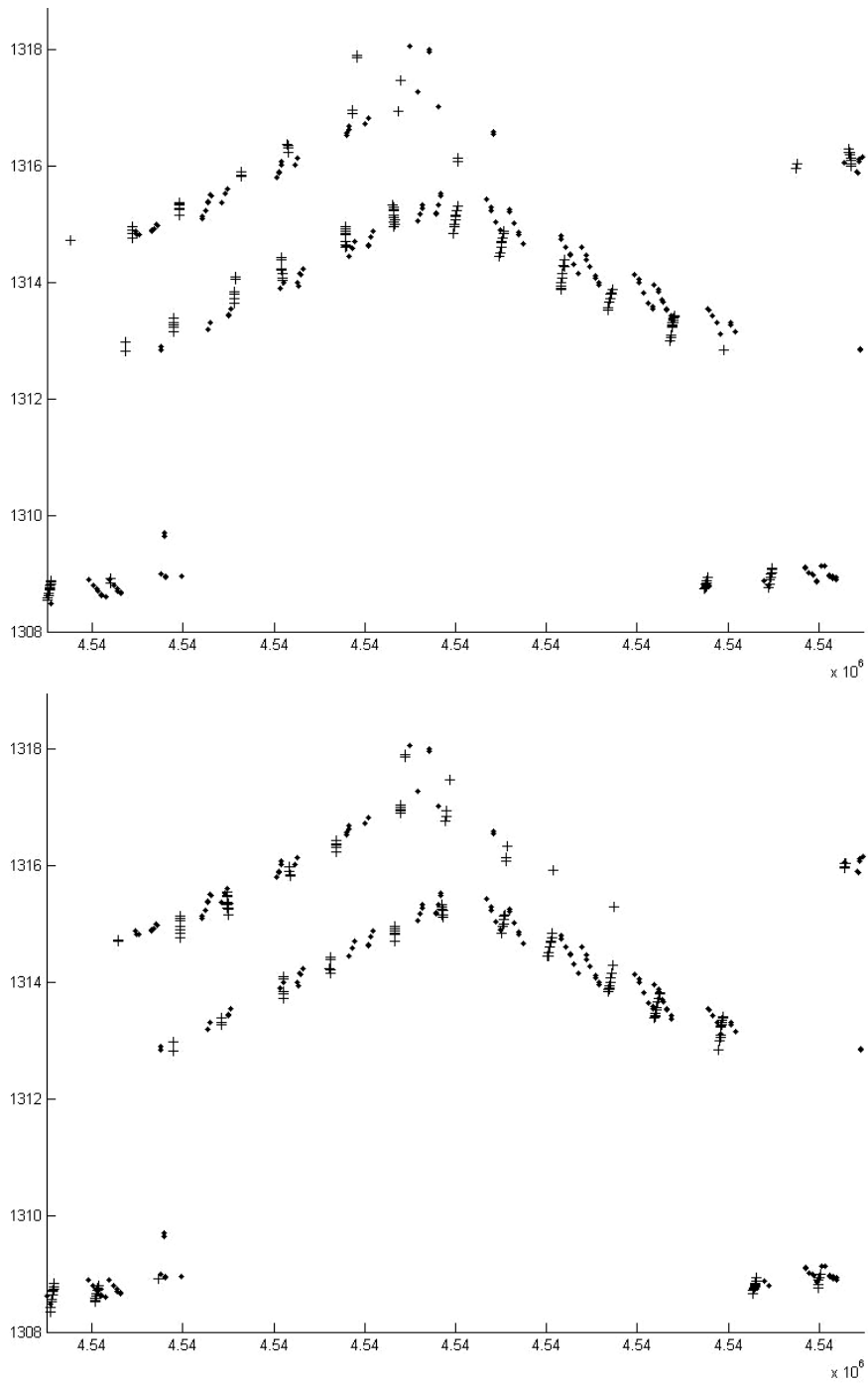


Figure3: Adjustment of the strips before (top) and after (bottom) application of the affine transformation. Dots represent data from the first flight. Crosses represent data from the second flight



## Acknowledgements

The UK Natural Environment Research Council are acknowledged for the provision of the image data as part of the Airborne Remote Sensing Facility 2006 Mediterranean Campaign, grant WM06-04.

J.A. Malpica, from the Department of Mathematics of the University of Alcalá, provided valuable suggestions. Comments from the anonymous reviewers are also acknowledged.

## References

- Crombaghs, M.J.E., Brügelmann, R. and de Min, E.J., 2000. On the adjustment of overlapping strips of laser altimeter height data. In: *International Archives of Photogrammetry and Remote Sensing*, vol. 33, part B3/1, pp. 224-231.
- Goodwin, N.R., Coops, N.C. and Culvenor, D.S. 2006. Assessment of forest structure with airborne LiDAR and the effects of platform altitude. *Remote Sensing of Environment*, 103, 140-152.
- Huising, E.J. and Gomes Pereira, L.M., 1998. Errors and accuracy estimates of laser data acquired by various laser scanning systems for topographic applications. *ISPRS Journal of Photogrammetry and Remote Sensing*, 53 (5), 241-261.
- Kager, H., 2004. Discrepancies between overlapping laser scanning strips – simultaneous fitting of aerial laser scanner strips. In *International Archives of Photogrammetry and Remote Sensing*, Vol. XXXV, B/1, pp. 555-560, Istanbul, Turkey.
- Lee, J., Yu, K., Kim, Y. and Habib, A.F., 2007. Adjustment of discrepancies between LiDAR data strips using linear features. *IEEE Geoscience and remote sensing letters*, 4 (3), 475-479.
- Lerma, J.L., 2002. Fotogrametría moderna: analítica y digital. Editorial U.P.V., pp. 427-477.
- Liu, D., Gong, P., Kelly, M. and Guo Q., 2006. Automatic registration of airborne images with complex local distortion. *Photogrammetric Engineering and Remote Sensing*, 72 (9), 1049-1059.
- Maas, H.-G. and Vosselman, 1999. Two algorithms for extracting buildings models from raw laser altimetry data. *ISPRS journal of Photogrammetry and Remote Sensing*, 54, 153-163
- Maas, H.-G., 2000. Least-squares matching with airborne laserscanning data in a TIN structure. In: *International Archives of Photogrammetry and Remote Sensing*, vol. 33, part B3/1, pp. 548-555.
- Maas, H.-G., 2001. On the use of reflectance data for laserscanner strip adjustment. In: *International Archives of Photogrammetry, Remote Sensing and Spatial Information Sciences*, vol. 34, part 3/w4, pp. 53-56.
- Maas, H.-G., 2002. Methods for measuring height and planimetry discrepancies in airborne laserscanner data. *Photogrammetric Engineering and Remote Sensing*, 68 (9), 933-940.
- Næsset, E., Gobakken, T., Holmgren, J., Hyyppä, H., Hyyppä, J., Maltamo, M., Nilsson, M., Olsson, H., Persson, A. and Söderman, U. (2004). Laser scanning of forest resources: The Nordic experience. *Scandinavian Journal of Forest Research*, 19, 482-499
- Pfeifer, N., Oude Elberink, S. and Filin, S., 2005. Automatic tie elements detection for laser scanner strip adjustment. In: *International Archives of Photogrammetry and Remote Sensing. Proceedings of Laserscanning*, vol. 36, part 3/w3, pp. 174-179.
- Prado, E. 2007. Mejoras en la evaluación y corrección de errores de registro en imágenes hiperespectrales AHS para estudios multitemporales. MSc Thesis. Departamento de Geografía. Universidad de Alcalá.
- Vosselman, G., 2002a. Strip offset estimation using linear features. In: *3<sup>rd</sup> international workshop on mapping geo-surficial processes using laser altimetry*, pp. 1-9.
- Vosselman, G., 2002b. On the estimation of planimetric offsets in laser altimetry data. In: *International Archives of Photogrammetry, Remote Sensing*, vol. 34, part 3A, pp. 375-380.